

Geographic potential of the world's largest hornet, *Vespa mandarinia* Smith (Hymenoptera: Vespidae), worldwide and particularly in North America

Claudia Nuñez-Penichet^{1,2}, Luis Osorio-Olvera^{2,3}, Victor H. Gonzalez^{1,4}, Marlon E. Cobos^{1,2}, Laura Jiménez^{1,2}, Devon A. DeRaad^{1,2}, Abdelghafar Alkhishe^{1,2}, Rusby G. Contreras-Díaz^{3,5}, Angela Nava-Bolaños², Kaera Utsumi¹, Uzma Ashraf⁶, Adeola Adeboje¹, A. Townsend Peterson^{1,2}, Jorge Soberon^{Corresp. 1,2}

¹ Department of Ecology & Evolutionary Biology, University of Kansas, Lawrence, KS, United States

² Biodiversity Institute, University of Kansas, Lawrence, Kansas, United States

³ Departamento de Matemáticas, Facultad de Ciencias, Universidad Nacional Autónoma de México, Ciudad de México, Ciudad de México, Mexico

⁴ Undergraduate Biology Program, University of Kansas, Lawrence, KS, United States

⁵ Posgrado en Ciencias Biológicas. Unidad de Posgrado, Universidad Nacional Autónoma de México, Ciudad de México, Ciudad de México, México

⁶ Department of Environmental Sciences and Policy, Lahore School of Economics, Lahore, Pakistan

Corresponding Author: Jorge Soberon

Email address: jsoberon@ku.edu

The Asian giant hornet (AGH, *Vespa mandarinia*) is the world's largest hornet, occurring naturally in the Indomalayan region, where it is a voracious predator of pollinating insects including honey bees. In September 2019, a nest of Asian giant hornets was detected outside of Vancouver, British Columbia and in May 2020 an individual was detected nearby in Washington state, indicating that the AGH could have successfully wintered in North America. Because hornets tend to spread rapidly and become pests, reliable estimates of the potential invasive range of *V. mandarinia* in North America are needed to assess likely human and economic impacts, and to guide future eradication attempts. Here, we assess climatic suitability for AGH in North America, and suggest that, without control, this species could establish populations across the Pacific Northwest and much of eastern North America. Predicted suitable areas for AGH in North America overlap broadly with areas where honey production is highest, as well as with species-rich areas for native bumble bees and stingless bees of the genus *Melipona* in Mexico, highlighting the economic and environmental necessity of controlling this nascent invasion.

1 **Geographic potential of the world's largest hornet, *Vespa mandarinia* Smith**
2 **(Hymenoptera: Vespidae), worldwide and particularly in North America**

3 Claudia Nuñez-Penichet^{1,2}, Luis Osorio-Olvera^{2,3}, Victor H. Gonzalez^{1,4}, Marlon E. Cobos^{1,2},
4 Laura Jiménez^{1,2}, Devon A. DeRaad^{1,2}, Abdelghafar Alkische^{1,2}, Rusby G. Contreras-Díaz^{3,5},
5 Angela Nava-Bolaños², Kaera Utsumi¹, Uzma Ashraf⁶, Adeola Adeboje¹, A. Townsend
6 Peterson^{1,2}, Jorge Soberon^{1,2*}

7 ¹Department of Ecology & Evolutionary Biology, University of Kansas, Lawrence, KS 66045
8 USA.

9 ²Biodiversity Institute, University of Kansas, Lawrence, KS 66045 USA.

10 ³Departamento de Matemáticas, Facultad de Ciencias, Universidad Nacional Autónoma de
11 México, Circuito Exterior s/n, Cd. Universitaria, 04510 Ciudad de México, México.

12 ⁴Undergraduate Biology Program, Haworth Hall, 1200 Sunnyside Ave. University of Kansas,
13 Lawrence, KS 66045 USA.

14 ⁵Posgrado en Ciencias Biológicas. Unidad de Posgrado, Edificio A, 1er Piso. Circuito de
15 Posgrados, Ciudad Universitaria, Delegación Coyoacán. C.P. 04510. Ciudad de México, México.

16 ⁶Department of Environmental Sciences and Policy, Lahore School of Economics, Lahore,
17 Pakistan.

18

19 *Corresponding Author: Jorge Soberon

20 Department of Ecology & Evolutionary Biology and Biodiversity Institute, University of Kansas,
21 1345 Jayhawk Blvd., Lawrence, Kansas 66045, USA. jsoberon@ku.edu

22

23 **ORCID:**

24 CNP: <https://orcid.org/0000-0001-7442-8593>

25 LOO: <https://orcid.org/0000-0003-0701-5398>

26 VHG: <https://orcid.org/0000-0002-4146-1634>

27 MEC: <https://orcid.org/0000-0002-2611-1767>

28 LJ: <https://orcid.org/0000-0002-6683-9576>

29 DAD: <https://orcid.org/0000-0003-3105-985X>

30 AbA: <https://orcid.org/0000-0003-2927-514X>

31 RGCD: <https://orcid.org/0000-0002-0569-8984>

32 ANB: <https://orcid.org/0000-0002-4371-5415>

33 KU: <https://orcid.org/0000-0001-5935-7299>

34 UA: <https://orcid.org/0000-0003-4319-9315>

35 AdA: <https://orcid.org/0000-0001-8513-7804>

36 ATP: <http://orcid.org/0000-0003-0243-2379>

37 JS: <https://orcid.org/0000-0003-2160-4148>

38 **ABSTRACT**

39 The Asian giant hornet (AGH, *Vespa mandarinia*) is the world's largest hornet, occurring
40 naturally in the Indomalayan region, where it is a voracious predator of pollinating insects
41 including honey bees. In September 2019, a nest of Asian giant hornets was detected outside of
42 Vancouver, British Columbia and in May 2020 an individual was detected nearby in Washington
43 state, indicating that the AGH could have successfully wintered in North America. Because
44 hornets tend to spread rapidly and become pests, reliable estimates of the potential invasive
45 range of *V. mandarinia* in North America are needed to assess likely human and economic
46 impacts, and to guide future eradication attempts. Here, we assess climatic suitability for AGH in
47 North America, and suggest that, without control, this species could establish populations across
48 the Pacific Northwest and much of eastern North America. Predicted suitable areas for AGH in
49 North America overlap broadly with areas where honey production is highest, as well as with
50 species-rich areas for native bumble bees and stingless bees of the genus *Melipona* in Mexico,
51 highlighting the economic and environmental necessity of controlling this nascent invasion.

52

53 **Keywords:** Asian giant hornet, dispersal simulation, ecological niche modeling, invasive
54 species, pollinator threats

55 Introduction

56 Invasive species represent major threats to biodiversity, as they can alter ecosystem
57 processes and functions (Pyšek & Richardson, 2010; Vilà et al., 2011), and often contribute to
58 the decline of imperiled species (e.g., Wilcove et al., 1998; Dueñas et al., 2018). The economic
59 damage to agriculture, forestry, and public health, resulting from invasive species totals nearly
60 US \$120 billion annually in the United States alone (Pimentel, Zuniga & Morrison, 2005), and
61 more than US \$172 million for Canada (Colautti et al., 2006).

62 Even in the midst of the global uncertainty and socio-economic distress resulting from
63 the COVID-19 pandemic, the recent detection of the Asian Giant Hornet (AGH, *Vespa*
64 *mandarina* Smith, Hymenoptera: Vespidae), in North America (Bérubé, 2020), received
65 significant public attention. This social insect is the world's largest hornet (2.5–4.5 cm body
66 length), and occurs naturally across Asia, including in India, Nepal, Sri Lanka, Vietnam, Taiwan,
67 and Japan, at elevations ranging between 850 and 1900 (Matsuura & Sakagami, 1973; Archer,
68 2008; Smith-Pardo, Carpenter & Kimsey, 2020). As in other temperate-zone social species,
69 annual colonies of the AGH, which may contain up to 500 workers, die at the onset of winter and
70 mated queens overwinter in underground cavities. After emerging in the spring, each queen starts
71 a new colony in a pre-existing cavity, typically in tree roots or an abandoned rodent nest (Archer,
72 2008). Like other species of *Vespa*, AGH is a voracious predator of insects, especially of bees
73 and other social Hymenoptera. Attacks on honey bee hives occur late in the development of the
74 hornet colony and prior to the emergence of reproductive individuals (males and new queens),
75 the timing of which depends on location (e.g., Matsuura & Sakagami, 1973; Matsuura, 1988;
76 Archer, 2008).

77 In its native range, AGH attacks several species of bees, some of which have developed
78 sophisticated defense mechanisms against attacks (Ono et al., 1995; Kastberger, Schmelzer &
79 Kranner, 2008; Fujiwara, Sasaki & Washitani, 2016). The best documented, colony-level defense
80 mechanism is in the Asiatic honey bee, *Apis cerana* Fabricius, which can detect site-marking
81 pheromones released by AGH scouts, and responds by engulfing a single hornet in a ball
82 consisting of up to 500 bees. The heat generated by the vibration of the bees' flight muscles, and
83 the resulting high levels of CO₂ from respiration effectively kill the hornet (Ono et al., 1995;
84 Sugahara, Nishimura & Sakamoto, 2012). In contrast, European honey bees (*A. mellifera* L.)
85 cannot detect and respond to AGH marking pheromones, and colonies are defenseless against
86 AGH attacks (McClenaghan et al., 2019). In Japan, as few as a dozen AGH can destroy a
87 European honey bee colony of up to 30,000 individuals, and extirpate thousands of beehives
88 annually (Matsuura & Sakagami, 1973).

89 In addition to the potential threat to the beekeeping industry (Alanis et al. 2020), the
90 introduction of AGH in North America is also concerning for public health. Their powerful
91 stings can induce severe allergic reactions or even death in hypersensitive individuals (Schmidt
92 et al., 1986; Yanagawa et al., 2007). Annually, 30-40 people die from AGH stings in Japan, most
93 as a result of anaphylaxis or sudden cardiac arrest (Matsuura & Sakagami, 1973); similar deadly
94 cases have been reported from China (Li et al., 2015).

95 Although invasive species are typically limited by dispersal ability and suitability of
96 novel environments, vespid hornets are well known for their invasive success and excellent
97 dispersal capacity (Beggs et al., 2011; Monceau, Bonnard & Thiéry, 2014). As such, the
98 introduction of AGH in the Pacific Northwest is already presenting a potentially serious
99 ecological and socio-economic risk in North America. Here, we use ecological niche modeling

100 (ENM) to detect areas of suitable environments for this species worldwide, with particular
101 emphasis on North America. We also use a dispersal simulation approach to detect potential
102 invasion paths of this species within North America. A similar methodology for projecting AGH
103 invasion potential has been implemented by Zhu et al. (2020); we build upon this framework by
104 introducing several modifications to the modelling approach, and investigating further the
105 potential ecological impact on the species richness of the genus *Bombus* and *Melipona* as well as
106 the possible economic effects of an AGH invasion in North America.

107 **Methods**

108 *Occurrence and environmental data*

109 We downloaded occurrence data for *V. mandarinia* from the Global Biodiversity
110 Information Facility database (GBIF; <https://www.gbif.org/>). We kept records from the species'
111 native range (Fig. 1) separate from non-native occurrences facilitated by human introduction. We
112 cleaned occurrences from the native distribution following Cobos et al. (2018) by removing
113 duplicates and records with inconsistent georeferencing (coordinates outside country limits, on
114 the sea, or missing, as recommended in the literature of data cleaning; Chapman, 2005). To avoid
115 model fitting derived from spatial autocorrelation and overdominance of specific regions due to
116 sampling bias, we thinned these records spatially in two ways: by geographic distance and by
117 density of records per country (Fig. 2). In the first case (distance-based thinning; Anderson,
118 2012), we excluded occurrences that were <50 km away from another occurrence record. In the
119 second thinning approach (country-density thinning), given radically different realities in
120 different countries as far as scientific activity that would detect the species, as well as reporting
121 and participating in global biodiversity information networks, we randomly reduced numbers of
122 occurrences in countries with the densest sampling, namely Japan, Taiwan, and South Korea

123 (from 30, 6, and 5, to 6, 2, and 2 occurrences, respectively), to match an approximate reference
124 density of India, Nepal, and China. We used the package `ellipsenm` (Cobos et al., 2020; available
125 at <https://github.com/marlonecobos/ellipsenm>) in R 3.6.2 (R Core Team, 2019) to clean and thin
126 the data. We retained 172 occurrence records for *V. mandarinia* after initial data cleaning, 49
127 records after the distance-based thinning approach, and 18 records after the country-density
128 thinning approach (Fig. 1). We then treated both data sets independently in all subsequent
129 analysis steps.

130 For environmental predictors, we used bioclimatic variables at 10' resolution (~18 km at
131 the Equator) from the MERRAclim database (Vega, Pertierra & Olalla-Tárraga, 2018). We
132 excluded four variables because they are known to contain spatial artifacts as a result of
133 combining temperature and humidity information (Escobar et al., 2014): mean temperature of
134 most humid quarter, mean temperature of least humid quarter, specific humidity mean of
135 warmest quarter, and specific humidity mean of coldest quarter. The 15 variables remaining were
136 masked to an area for model calibration (**M**, see Ecological niche modeling).

137 These 15 variables were further processed into two subsets, each used separately in all
138 subsequent analyses. One set consisted of submitting the variables to a principal component
139 analysis (PCA) to reduce dimensionality and multicollinearity. The other set was created with the
140 raw environmental variables that had a Pearson's correlation coefficient ≤ 0.85 measured in the
141 calibration area, choosing the most biologically relevant or interpretable variables based on our
142 knowledge of AGH natural history (Simões et al., 2020). As a result of this selection process, we
143 obtained six raw variables: isothermality (BIO3), maximum temperature of warmest month
144 (BIO5), minimum temperature of coldest month (BIO6), temperature annual range (BIO7),
145 specific humidity of most humid month (BIO13), and specific humidity of least humid month

146 (BIO14). The PCA was performed with the raw variables masked to the M area, and principal
147 components for the entire world were obtained by transforming raw variables (at world extent)
148 using the scaling and rotations from the PCA obtained for M. Projecting the PCA results from
149 the accessible area to the entire world warranties that values are comparable and prevents further
150 problems when models are projected. For further analyses, we kept the first four PC axes, as they
151 explained 97.9% of the cumulative variance (Figure S1). All analyses were done in R;
152 specifically, raster processing was done using the packages raster (Hijmans et al., 2020), rgeos
153 (Bivand et al., 2020b), and rgdal (Bivand et al., 2020a); PCA was done using the ntbox package
154 (Osorio-Olvera et al., 2020).

155

156 *Ecological niche modeling*

157 To identify a calibration area (ostensibly equivalent to **M**; Owens et al., 2013) for our
158 models, we considered a region contained within a buffer of 500 km around the known
159 occurrence records after the 50 km thinning process (Fig. 1). This distance was selected
160 considering the species' dispersal ability (Matsuura & Sakagami, 1973; APHIS, 2020a). We used
161 all pixels in **M** (15,411) as the background across which to calibrate the models.

162 Given uncertainty deriving from specific treatments of occurrence records and
163 environmental predictors in ecological niche modeling (Alkische et al., 2020), we calibrated
164 models via four distinct schemes: (1) using raw variables and distance-based thinned
165 occurrences, (2) using PCs and distance-based thinned occurrences, (3) using raw environmental
166 variables and country-density thinned occurrences, and (4) using PCs and country-density
167 thinned occurrences (Fig. 2). For each scheme, we calibrated models five times, each time

168 randomly selecting 50% of the occurrences for calibrating models (random k-fold evaluation,
169 where $k = 5$), and using the remaining records for testing (Cobos et al., 2019a).

170 Each process of model calibration consisted of creating and evaluating candidate models
171 using Maxent (Phillips, Anderson & Schapire, 2006; Phillips et al., 2017). Since many choices
172 are needed to parameterize Maxent (Merow, Smith & Silander, 2013), we chose distinct
173 parameter settings: 10 regularization multiplier values (0.10, 0.25, 0.50, 0.75, 1, 2, 3, 4, 5, 6),
174 eight feature classes (lq, lp, lqp, qp, q, lqpt, lqpth, lqph, where l is linear, q is quadratic, p is
175 product, t is threshold, and h is hinge), and all combinations of more than two predictor variables
176 (Cobos et al., 2019b; Table S1-S2). This resulted in a total of 4560 models using raw variables
177 and 880 using PCs that were tested, in tandem with the two subsets of occurrence data described
178 above. We assessed model performance using partial ROC (for statistical significance; Peterson,
179 Papeş & Soberón, 2008), omission rates ($E = 5\%$, for predictive ability; Anderson, Lew &
180 Peterson, 2003), and Akaike Information Criterion corrected for small sample sizes (AICc, for
181 model complexity; Warren & Seifert, 2011). We selected models with $\Delta AICc \leq 2$ (Cobos et
182 al., 2019a) from those that were statistically significant and had omission rates below 5%.

183 After model calibration, we created models with the selected parameter values, using all
184 occurrences after the corresponding thinning process, with 10 bootstrap replicates, cloglog
185 output (Phillips et al., 2017), and model transfers using three types of extrapolation (free
186 extrapolation, extrapolation with clamping, no extrapolation; Owens et al., 2013). Not all
187 calibration processes identified models that met all three criteria of model selection; we did not
188 consider those models in further analyses (Fig. 2; Table 1). As a final evaluation step, we
189 binarized all model replicates given a modified least presence (5% of omission) and then tested
190 whether each replicate of the selected models was able to anticipate the known invasive records

191 of the species in the Americas (British Columbia, Canada; Washington, USA). For each scheme,
192 using only those model replicates that met the selection criteria and correctly predicted
193 independent occurrences (known invaded localities in North America; independent testing), we
194 created a consensus per sample and two types of final consensus: (1) a median of the medians
195 obtained for each parameterization (continuous), and (2) the sum of all suitable areas derived
196 from binarizing each replicate using a modified least presence (5% omission) threshold (this
197 represents the number of coincidences; Pearson et al. 2007; Fig. 2). Our exploration of different
198 modeling pipelines allowed us to highlight how different methodologies produce different
199 results.

200 As we transferred models to the entire world, we used the mobility-oriented parity metric
201 (MOP; Owens et al., 2013) to detect areas where strict or combinational extrapolation risks could
202 be expected, given the presence of non-analogous conditions with respect to the environments
203 manifested across the calibration area. The areas where extrapolation risks were detected using
204 MOP were deleted from our binary results (suitable areas) to avoid potentially problematic
205 interpretations based on extrapolative situations. Model calibration, production of selected
206 models with replicates, and MOP analyses were done in R using the package kuenm (Cobos et
207 al., 2019a); raster processing and independent testing of models were done using the package
208 raster in R.

209

210 *Dispersal simulations*

211 We used the binary outputs from the final consensus models (suitable and unsuitable
212 areas, without areas of strict extrapolation) to simulate invasion dynamics of the AGH. All

213 simulations were started from the Pacific Northwest, from sites already known to be occupied by
214 the AGH. The simulations were performed using the cellular automaton dynamic model included
215 in the bam R package (Osorio-Olvera & Soberón, 2020; available at
216 <https://github.com/luismurao/bam>). Under this discrete model, given an occupied area at time t ,
217 two layers of information are needed to obtain the occupied area at time $t + 1$: (i) the binary layer
218 of suitability for the species, and (ii) a connectivity matrix determined by the species' ability to
219 reach neighboring cells in one time unit (known as “Moore’s neighborhood”; Gray et al., 2003,
220 that defines patches that are connected by dispersal). At each step, each of the suitable cells can
221 be either occupied or not by the species. If a cell is occupied, adjacent cells can be visited by the
222 species, and if suitable, they become occupied. This method is similar to the one implemented in
223 the MigClim R package (Engler, Hordijk & Guisan, 2012), but uses a simpler dispersal kernel
224 and parameterization.

225 With each of the final consensus models for *V. mandarinia*, we performed a set of
226 simulations in which we explored different degrees of connectivity (1, 2, 4, 8, 10, and 12
227 neighbor cells, pixels per unit time) and different suitability thresholds (10 equidistant levels
228 from 3–10% of the presence points to explore variability in sensitivity to the amount of area
229 classified as suitable) to create the binary maps. Since no information is available about dispersal
230 capacities of queens of *V. mandarinia*, all simulations were done with 200 arbitrary time steps
231 that ensure reaching a steady state. In the end, we visualized the simulation results by summing
232 the occupied distribution layers obtained from each set of simulations. A value of 100 in these
233 final layers means that the species reached that cell in 100% of the simulations, whereas a value
234 of 0 means that the species never reached that cell. Further details regarding the simulation
235 processes can be found in the Supplementary Information.

236

237 *Honey production and native bee richness in North America*

238 To explore potential ecological and economic impacts of the invasion of the AGH in
239 North America, we explored annual, state-level production of honey (for Mexico, United States,
240 and Canada) as well as species richness of bumble bees (*Bombus* Latreille) and stingless bees of
241 the genus *Melipona* Illiger in Mexico and the United States. We extracted data on 2016 honey
242 production (in US dollars) for the United States from the U.S. Department of Agriculture
243 (USDA; available at [https://quickstats.nass.usda.gov/#4A0314DA-F3E5-3B06-ADD1-
244 CA8032FBD937](https://quickstats.nass.usda.gov/#4A0314DA-F3E5-3B06-ADD1-CA8032FBD937)), from the Instituto Nacional de Estadística, Geografía e Informática (INEGI)
245 for Mexico (<https://atlasapi2019.github.io/cap4.html>), and from the government of Canada
246 website ([https://www.agr.gc.ca/eng/horticulture/horticulture-sector-reports/statistical-overview-
247 of-the-canadian-honey-and-bee-industry-2018/?id=1571143699779](https://www.agr.gc.ca/eng/horticulture/horticulture-sector-reports/statistical-overview-of-the-canadian-honey-and-bee-industry-2018/?id=1571143699779)) for Canada. For native
248 species richness, we obtained a list of species of bumble bees and stingless bees of the genus
249 *Melipona* that occur in Mexico and the United States from Discover Life
250 (<https://www.discoverlife.org/>) and downloaded their occurrence data from GBIF. We chose
251 these bee taxa as likely targets of AGH because the species in these groups are of similar body
252 size and behavior to the typical prey of these hornets: they are social insects that form annual or
253 perennial colonies that can have a few hundreds to as many as 10,000 individuals (Cueva del
254 Castillo, Sanabria-Urbán & Serrano-Meneses, 2015; Viana et al., 2015), and store honey and
255 pollen inside their nests (Michener, 2000). To summarize species richness of these two genera,
256 we created a presence absence matrix (PAM; Arita et al., 2008) for North America, based on
257 geographic coordinates of occurrence data, with a pixel size of one degree. The PAM was

258 created in R with the package biosurvey (Nuñez-Penichet et al., 2020; available at
259 <https://github.com/claununez/biosurvey>).

260 To assure transparency and reproducibility of our work, we include an Overview, Data,
261 Model, Assessment, and Prediction protocol (ODMAP; Zurell et al., 2020) in our supplementary
262 materials. This metadata summary provides a detailed key to the steps of our analyses. The data
263 and R code used in this research are openly available at <http://hdl.handle.net/1808/30602> and
264 <https://github.com/townpeterson/vespa> repositories, respectively.

265

266 **Results**

267 *Model calibration*

268 The number of models that met the selection criteria was considerably smaller than the
269 total number of models tested (Table 1, see Supplemental information for more details of the
270 calibration results). The calibration schemes including raw variables had fewer models selected
271 than those using PCs (11, 19, 6, 15 models selected for raw/distance-thinned, PC/distance-
272 thinned, raw/country-density, and PC/country-density, respectively). Not all replicates of
273 selected models anticipated the *V. mandarinia* invaded areas in North America successfully, so
274 we kept only those that predicted all known invasive records. The number of replicates retained
275 varied among distinct calibration schemes and types of extrapolation used (Table 1).

276

277 *Ecological niche model predictions*

278 In our models, areas predicted as suitable for the AGH varied among calibration schemes,
279 in both extension and geographic pattern (Fig. 3, Figures S2-S4). The differences are
280 conspicuous between the two types of thinning approaches, which resulted in models created
281 with different numbers of occurrence records. Models with country-density thinning (18 records)
282 resulted in broad predicted suitable areas worldwide, with areas of higher values of suitability
283 concentrated in tropical regions (Fig. 3, Figures S2-S4). In contrast, models created with the
284 greater number of occurrences (49 records) from the geographic distance thinning predicted
285 more patches of suitable areas across large extensions of Southeast Asia, Europe, West Africa,
286 Central America, northern South America, and the Pacific Northwest and southeastern United
287 States (Fig. 3, Figures S2-S4). In the calibration area, the areas detected with high levels of
288 suitability were larger in the scheme with geographic distance thinned occurrences and the raw
289 variables and smaller in the predictions obtained with the country-density thinned occurrences
290 and the PCs as environmental predictors (Fig. 3). In all schemes, the two northernmost
291 occurrence points of this species in China were accorded relatively low levels of suitability (Fig.
292 3). Predicted suitable areas for this hornet worldwide were also different among types of
293 extrapolation considered in this study, especially as regards its distribution size rather than
294 location (Figures S2-S4).

295 In North America, across multiple model calibration schemes, our various models agreed
296 in predicting suitable areas for AGH in the Pacific region of southwestern Canada, the Pacific
297 Northwest, the southeastern United States, and from central Mexico south to southernmost
298 Panama (Fig. 4). Our model calibration schemes also agreed in identifying the Rocky Mountains
299 and Great Plains as unsuitable for this species (Fig. 4).

300 The proportion of area identified as suitable varied among the data thinning schemes. In
301 the case of models created with raw variables, the proportion was 0.171 and 0.164 for spatially
302 thinned and country-density thinned records, respectively. When PCs were used, suitable
303 proportions were 0.248 and 0.239, for spatially thinned and country-density thinned records,
304 respectively (Table S3).

305 *Extrapolation risks in model projections*

306 The pattern of areas detected with risk of extrapolation was similar worldwide between
307 thinning methods, but different between raw variables and PCs (Fig. 5, Figure S8). Most tropical
308 areas predicted as suitable were identified as regions with high extrapolation risk (Figure S8).
309 For raw variables, the areas with extrapolation risk in North America included most of Canada
310 and Alaska, whereas for PCs areas with extrapolation risk included large portions of Mexico and,
311 the central-southwestern United States, as well as the islands north of Hudson Bay in Canada
312 (Fig. 5).

313

314 *Simulations of potential invasion*

315 The simulations of potential sequences of colonization and dispersal of AGH in North
316 America, starting from the known invaded localities, showed agreement among calibration
317 schemes in predicting an invasion across the Pacific Northwest from southernmost Alaska to
318 southernmost California in the United States (Fig. 6). In contrast, we found that the dispersal
319 distance required to invade all the way to the East Coast of North America varied among
320 calibration schemes. In the schemes using raw variables, the route of invasion to reach the East
321 Coast goes from the Pacific Northwest down to California and Mexico, and then up the East

322 Coast of North America. A dispersal distance of 10 cells (where each cell represents ~18 km)
323 was enough to reach the East Coast (see left panels in Fig. 6). For the scheme using the 50 km
324 spatially-thinned occurrences and PCs, the invasion follows a more direct route from the Pacific
325 Northwest to the East Coast that goes through the United States, and the required dispersal
326 distance to reach the East Coast was only 4 cells (top right panel in Fig. 6). Finally, in the case of
327 country-density thinned occurrences and PCs, the invasion goes from the Pacific Northwest
328 through Canada to the Atlantic, and then down the East Coast to the United States. A distance of
329 8 cells was needed to make this invasion route possible (bottom right panel in Fig. 6).

330

331 *Honey production and native bee richness*

332 The areas in North America that our models identified as highly suitable for AGH
333 overlapped broadly with the states where honey production is highest. This overlap was
334 particularly noticeable in southern Mexico and in some states of the Pacific Northwest and
335 eastern US (Fig. 7). We found a similar pattern with the species richness of *Bombus* and
336 *Melipona*.

337

338 Discussion

339 The patterns of suitability that we found in North America across multiple input data
340 processing schemes are broadly concurrent with the results obtained by Zhu et al. (2020) (Fig. 6),
341 who used an ensemble modeling approach for the potential invasion of AGH. This concordance
342 with the results of Zhu et al. (2020) (both among our selected models, and between our models

343 and the ensemble models), gives us confidence that the Pacific Northwest and southeastern
344 United States represent suitable areas for AGH. In contrast with the results of Zhu et al. (2020),
345 however, our dispersal simulations indicate a larger potential invasion area in the United States,
346 with the AGH potentially crossing to eastern North America via a southern invasion route,
347 through Mexico and Texas; a southeast-ward route crossing Idaho, Wyoming, and Colorado; or a
348 northern route across Canada and the Great Lakes region (Fig. 6).

349 Quantifying the probability of the AGH following any one of the individual dispersal
350 routes presented would require precise quantification of dispersal ability, and discerning the real-
351 world validity of each of the four modeling outcomes. Instead of attempting to guess, we present
352 several models that offer multiple plausible invasion scenarios. Across all scenarios presented,
353 the AGH is expected to establish populations along the coastal Pacific Northwest via short-
354 distance dispersal, and it is likely to invade the southeastern United States if it has even moderate
355 dispersal potential (Fig. 6). It is important to note that these potential invasion routes consider
356 only the natural dispersal ability of this hornet, and do not take into account the effect of
357 potential accidental human-aided dispersal through the transport of soil and wood, where
358 fertilized queen AGHs overwinter (Archer, 1995). Such unwitting human-aided dispersal is a
359 serious concern, as it could potentiate a rapid invasion of this hornet to environmentally suitable,
360 yet currently isolated places across North America. Our simulations allowing AGH to disperse to
361 larger numbers of neighbor cells are perhaps a good illustration of what could be expected if
362 dispersal events to very long distances occur.

363 Contrasts between our prediction of extensive invasion potential, and Zhu et al.'s (2020)
364 more conservative predictions, arise from Zhu et al.'s (2020) use of MigClim (Engler, Hordijk &
365 Guisan, 2012) to model dispersal of the AGH in western North America. MigClim is a cellular

366 automaton platform that models the state of grid cells as occupied or unoccupied. Although we
367 used the same modelling technique, our dispersal kernel is a much simpler “Moore
368 Neighborhood” (Gray et al., 2003) approach, in which cells surrounding an occupied focal cell
369 (to $1, 2, \dots, d$ neighbors) may become occupied, depending on their suitability. MigClim instead
370 assumes a probabilistic contagion model that requires parameter estimates for number of
371 propagules, and short- and long-distance-decay rates. Given the lack of empirical data to inform
372 values for those parameters, we prefer a simpler algorithm to explore how connected clusters of
373 suitable cells are across different values of the single parameter d . Another factor resulting in
374 these differences is the number of simulation steps used in our approach (200). From a biological
375 perspective, this implies that 200 dispersal events resulting in colonization of suitable cells
376 happened. Although this number may appear excessive, it gives a view of a scenario in which no
377 action is taken to prevent AGH invasion in North America and the species builds to large local
378 populations. For a more conservative view of the expected invasion, one could concentrate in
379 areas with high values of suitability on the layers obtained from our simulations.

380 The areas in North America that our models identified as highly suitable for this hornet
381 overlap broadly with the states where honey production is highest, and species richness of
382 *Bombus* and *Melipona* are highest (Fig. 7). These results give credence to public concerns that, if
383 established, the AGH could pose a serious economic threat to the beekeeping industry in Oregon,
384 northern California, Georgia, Alabama, and Florida. In the United States alone, the European
385 honey bee provides at least \$15 billion worth of pollination services and generates between \$300
386 and 500 million in harvestable honey and other products each year (Calderone, 2012). In
387 Mexico, impacts on the honey bee industry are also expected in tropical areas of the country that
388 have suitable areas for the AGH, particularly in the states of Yucatán, Campeche, and Quintana

389 Roo. Beekeepers in the United States and Mexico may have to adopt mitigation practices to
390 avoid serious losses, such as those developed by Japanese beekeepers including the use of
391 protective screens or traps at the hive entrance that can exclude AGHs based on body size
392 (Matsuura & Sakagami, 1973; Mahdi, Glaiim & Ibrahim, 2008). Potential establishment of the
393 AGH in North America adds an additional layer of environmental and economic stress to a
394 beekeeping industry already suffering from high annual hive mortality rates resulting from the
395 combined effects of pesticides, diseases, and poor nutrition (Goulson et al., 2015).

396 The ecological impact of AGH on the local bee fauna is more challenging to predict than
397 the economic impact on honey production, because it is not clear which native bee species would
398 be particularly targeted by AGH in North America. We explore *Bombus* and *Melipona* species as
399 likely prey candidates of AGH because, among the >4000 bee species occurring in this region
400 (Ascher & Pickering, 2020), these two groups of bees are social, locally abundant, and make
401 annual or perennial colonies (Michener, 2007; Cueva del Castillo, Sanabria-Urbán &
402 Serrano-Meneses, 2015; Viana et al., 2015). Thus, they may represent predictable food sources
403 for the AGH. It is crucial to consider this potential threat because both *Bombus* and *Melipona*
404 bees are important pollinators that have already experienced population losses and local
405 extirpations, reflecting changes in landscape and agricultural intensification (Brown & Albrecht,
406 2001; Cameron et al., 2011). Furthermore, these species, as well as the European honey bee, lack
407 behavioral responses to prevent predation by the AGH (Matsuura & Sakagami, 1973;
408 McClenaghan et al., 2019), because they have no shared evolutionary history with the AGH, and
409 are thus vulnerable to its predatory and antagonistic behavior. The economic and cultural
410 importance of *Melipona* species in America is well-documented, particularly in the Yucatan
411 Peninsula in Mexico, where these bees have been traditionally raised for honey and were even

412 considered gods outright in Mayan times (Ayala, Gonzalez & Engel, 2013; Quezada-Euán et al.,
413 2018). It is important to mention, however, that the risk to *Melipona* species may be lower than
414 that to *Bombus* species because entrances to the hives of some species of *Melipona* are narrow,
415 allowing a single bee to pass at a time (Couvillon et al., 2007), unlike the entrances to the hives
416 of honey bees and many bumble bees, which are wider.

417 The AGH is not the first Hymenoptera to invade North America, and species of *Vespa* are
418 well-known for their invasive success and excellent dispersal capacity (Beggs et al., 2011;
419 Monceau, Bonnard & Thiéry, 2014). Additionally, the European hornet, *Vespa crabro* L., a
420 Eurasian species that was accidentally introduced to North America in the 1800s, occupies a
421 similar invasive range in the United States (Smith et al. 2020). The solitary giant resin bee,
422 *Challomegachile sculpturalis* is an Asian taxon which was recently introduced in the United
423 States. Only 15 years after its initial detection near Baltimore, Maryland, this species had
424 invaded most of the southeastern United States (Hinojosa-Díaz et al., 2005). These examples
425 indicate considerable precedent for hornet invasion and establishment in the southeastern United
426 States, but the AGH poses a unique biodiversity risk as a direct predator of bees. Because the
427 Pacific Northwest is consistently predicted as suitable for the AGH, preventing further
428 establishment and spread of recently detected introduced populations near Seattle and Vancouver
429 is essential. The cause of the introduction is unknown, although, the Department of Agriculture
430 speculates that it may have been unlawfully introduced for medicinal purposes (APHISb). If
431 these introduced individuals are not eradicated, they may flourish under the suitable climatic
432 conditions, establishing many more colonies that will be difficult to control. Preventing
433 establishment of the AGH in the Pacific Northwest is especially critical because an established
434 AGH population in the Pacific Northwest would provide a source population for potential long-

435 range dispersers that could use multiple potential invasion routes (Fig. 6) to reach suitable habitat
436 in the eastern United States, facilitating full-scale invasion. In light of this, we recommend
437 official monitoring protocols for the vulnerable Pacific Northwest region, and encourage citizen-
438 science monitoring efforts, duly informed by APHIS (2020) data on the identity of the AGH,
439 which may be the fastest and most effective way to detect potential range expansions.

440 Although AGH is primarily found in temperate areas in its native range, some of its
441 populations reach subtropical regions like Taiwan (Archer, 2008), which indicates a broad
442 temperature tolerance. This southern part of the species' native range might explain why our
443 models predicted suitable areas in South America, Africa, and elsewhere (Figure 2S-S7).
444 Although temperature is a critical factor that determines the abundance and distribution of
445 organisms (Sunday, Bates & Dulvy, 2012), factors such as desiccation resistance may be equally
446 important for some species. For example, for ants and some bees, desiccation tolerance is a good
447 predictor of species' distributions (Bujan, Yanoviak & Kaspari, 2016; Burdine & McCluney,
448 2019). For example, humidity is important for the regulation of temperature in nests of the
449 European hornet (Klingner et al., 2005) and, in some species of stingless bees, regulation of
450 humidity appears to be more important than regulation of temperature to maintain colony health
451 (Ayton et al., 2016). Unfortunately, heat and desiccation tolerances, factors that might improve
452 predictions of this species' distributional potential, are unknown for the AGH. In other hornets,
453 subtropical populations tend to have longer population cycles than temperate populations
454 (Archer, 2008), so negative impacts of an AGH invasion may be stronger in tropical or
455 subtropical areas.

456 In summary, our modeling approach allowed us to recognize how predicted suitable
457 areas can be depending on distinct schemes of data treatment. We showed that this variability

458 can derive from crucial decisions made during the initial steps of ecological niche modeling
459 exercises. These results highlight the importance of such initial decisions, as well as the need to
460 recognize sources of variability in predictions of suitability. This point is of special importance
461 in predicting the potential for expansion of invasive species, as uncertainty increases when
462 models are transferred to areas where environmental conditions are different. Our analyses and
463 simulations revealed the potential of the AGH to invade large areas in North America and the
464 likely paths of such an invasion. We also showed that predicted suitable areas for the AGH
465 overlap broadly with those where honey production is highest in the United States and Mexico,
466 as well as with species-rich areas for bumble bees and stingless bees. These results bring light to
467 the potential implications of uncontrolled dispersal of the AGH to suitable environments in
468 North America, and highlight the need for rapid eradication actions to mitigate potential
469 biodiversity and economic losses.

470

471 **Acknowledgments**

472 We would like to thank the members of the KUENM group for their support in the development
473 of this manuscript. We also thank Allan Smith-Pardo for letting us use the photograph of AGH in
474 lateral view (Fig. 1B). ANB would like to thank Secretaría de Educación, Ciencia, Tecnología e
475 Innovación de la Ciudad de México.

476

477 **References**

478 APHIS. 2020a. New pest response guidelines: *Vespa mandarinia*. U.S. Department of
479 Agriculture, Animal and Plant Health Inspection Service, Plant Protection and

- 480 Quarantine.
- 481 APHIS. 2020b. Asian Giant Hornet. U.S. Department of Agriculture, National Invasive Species
482 Information Center. [https://www.invasivespeciesinfo.gov/terrestrial/invertebrates/asian-](https://www.invasivespeciesinfo.gov/terrestrial/invertebrates/asian-giant-hornet)
483 [giant-hornet](https://www.invasivespeciesinfo.gov/terrestrial/invertebrates/asian-giant-hornet).
- 484 Alaniz AJ, Carvajal MA, Vergara PM, 2020. Giants are coming? Predicting the potential spread
485 and impacts of the giant Asian hornet (*Vespa mandarinia*, Hymenoptera: Vespidae) in the
486 United States. *Pest Management Science*. DOI: 10.1002/ps.6063.
- 487 Alkishe A, Cobos ME, Peterson AT, Samy AM. 2020. Recognizing sources of uncertainty in
488 disease vector ecological niche models: an example with the tick *Rhipicephalus*
489 *sanguineus* sensu lato. *Perspectives in Ecology and Conservation*. DOI:
490 10.1016/j.pecon.2020.03.002.
- 491 Anderson RP. 2012. Harnessing the world's biodiversity data: promise and peril in ecological
492 niche modeling of species distributions. *Annals of the New York Academy of Sciences*
493 1260:66–80. DOI: 10.1111/j.1749-6632.2011.06440.x.
- 494 Anderson RP, Lew D, Peterson AT. 2003. Evaluating predictive models of species' distributions:
495 criteria for selecting optimal models. *Ecological Modelling* 162:211–232. DOI:
496 10.1016/S0304-3800(02)00349-6.
- 497 Archer ME. 1995. Taxonomy, distribution and nesting biology of the *Vespa mandarinia* group
498 (Hym., Vespinae). *Entomologist's Monthly Magazine* 131:47–53.
- 499 Archer ME. 2008. Taxonomy, distribution and nesting biology of species of the genera *Provespa*
500 *Ashmead* and *Vespa* Linnaeus (Hymenoptera, Vespidae). *Entomologist's Monthly*
501 *Magazine* 144:69–101.
- 502 Arita HT, Christen JA, Rodríguez P, Soberón J. 2008. Species diversity and distribution in

- 503 presence-absence matrices: mathematical relationships and biological implications.
504 *American Naturalist* 172:519–532. DOI: 10.1086/590954.
- 505 Ascher JS, Pickering J. 2020. Discover life bee species guide and world checklist (Hymenoptera:
506 Apoidea: *Anthophila*). Available at
507 https://www.discoverlife.org/mp/20q?guide=Apoidea_species (accessed July 1, 2020).
- 508 Ayala R, Gonzalez VH, Engel MS. 2013. Mexican stingless bees (Hymenoptera: Apidae):
509 diversity, distribution, and indigenous knowledge. In: Vit P, Pedro SRM, Roubik D eds.
510 *Pot-Honey: A Legacy of Stingless Bees*. New York, NY: Springer, 135–152. DOI:
511 10.1007/978-1-4614-4960-7_9.
- 512 Ayton S, Tomlinson S, Phillips RD, Dixon KW, Withers PC. 2016. Phenophysiological variation
513 of a bee that regulates hive humidity, but not hive temperature. *Journal of Experimental*
514 *Biology* 219:1552–1562. DOI: 10.1242/jeb.137588.
- 515 Barve N, Barve V, Jiménez-Valverde A, Lira-Noriega A, Maher SP, Peterson AT, Soberón J,
516 Villalobos F. 2011. The crucial role of the accessible area in ecological niche modeling
517 and species distribution modeling. *Ecological Modelling* 222:1810–1819. DOI:
518 10.1016/j.ecolmodel.2011.02.011.
- 519 Beggs JR, Brockerhoff EG, Corley JC, Kenis M, Masciocchi M, Muller F, Rome Q, Villemant
520 C. 2011. Ecological effects and management of invasive alien Vespidae. *BioControl*
521 56:505–526. DOI: 10.1007/s10526-011-9389-z.
- 522 Bérubé C. 2020. Giant alien insect invasion averted Canadian beekeepers thwart apicultural
523 disaster (... or at least the zorn-bee apocalypse). *American Bee Journal*:209–214.
- 524 Bivand R, Keitt T, Rowlingson B, Pebesma E, Sumner M, Hijmans R, Rouault E, Warmerdam F,
525 Ooms J, Rundel C. 2020a. *rgdal: Bindings for the “geospatial” data abstraction library*.

- 526 <https://cran.r-project.org/web/packages/rgdal/index.html>.
- 527 Bivand R, Rundel C, Pebesma E, Stuetz R, Hufthammer KO, Giraudoux P, Davis M, Santilli S.
528 2020b. *rgeos: Interface to geometry engine - open source ('GEOS')*. [https://cran.r-](https://cran.r-project.org/web/packages/rgeos/index.html)
529 [project.org/web/packages/rgeos/index.html](https://cran.r-project.org/web/packages/rgeos/index.html).
- 530 Brown JC, Albrecht C. 2001. The effect of tropical deforestation on stingless bees of the genus
531 *Melipona* (Insecta: Hymenoptera: Apidae: Meliponini) in central Rondonia, Brazil.
532 *Journal of Biogeography* 28:623–634. DOI: 10.1046/j.1365-2699.2001.00583.x.
- 533 Bujan J, Yanoviak SP, Kaspari M. 2016. Desiccation resistance in tropical insects: causes and
534 mechanisms underlying variability in a Panama ant community. *Ecology and Evolution*
535 6:6282–6291. DOI: 10.1002/ece3.2355.
- 536 Burdine JD, McCluney KE. 2019. Differential sensitivity of bees to urbanization-driven changes
537 in body temperature and water content. *Scientific Reports* 9:1643. DOI: 10.1038/s41598-
538 018-38338-0.
- 539 Cameron SA, Lozier JD, Strange JP, Koch JB, Cordes N, Solter LF, Griswold TL. 2011. Patterns
540 of widespread decline in North American bumble bees. *Proceedings of the National*
541 *Academy of Sciences USA* 108:662–667. DOI: 10.1073/pnas.1014743108.
- 542 Chapman AD. 2005. Principles and methods of data cleaning. Copenhagen, GBIF.
- 543 Cobos ME, Jiménez L, Nuñez-Penichet C, Romero-Alvarez D, Simões M. 2018. Sample data
544 and training modules for cleaning biodiversity information. *Biodiversity Informatics*
545 13:49–50. DOI: 10.17161/bi.v13i0.7600.
- 546 Cobos ME, Osorio-Olvera L, Soberón J, Peterson AT, Barve V, Barve N. 2020. *ellipsenm:*
547 *Ecological niche characterizations using ellipsoids*.
548 <https://github.com/marlonecobos/ellipsenm>.

- 549 Cobos ME, Peterson AT, Barve N, Osorio-Olvera L. 2019a. kuenm: an R package for detailed
550 development of ecological niche models using Maxent. *PeerJ* 7:e6281. DOI:
551 10.7717/peerj.6281.
- 552 Cobos ME, Peterson AT, Osorio-Olvera L, Jiménez-García D. 2019b. An exhaustive analysis of
553 heuristic methods for variable selection in ecological niche modeling and species
554 distribution modeling. *Ecological Informatics* 53:100983. DOI:
555 10.1016/j.ecoinf.2019.100983.
- 556 Colautti RI, Bailey SA, Van Overdijk CD, Amundsen K, MacIsaac H J. 2006. Characterized and
557 projected costs of nonindigenous species in Canada. *Biological Invasions* 8(1):45–59.
- 558 Couvillon MJ, Wenseleers T, Imperatriz-Fonseca VL, Nogueira-Neto P, Ratnieks FLW. 2007.
559 Comparative study in stingless bees (Meliponini) demonstrates that nest entrance size
560 predicts traffic and defensivity. *Journal of Evolutionary Biology* 21:194–201. DOI:
561 10.1111/j.1420-9101.2007.01457.x.
- 562 Cueva del Castillo R, Sanabria-Urbán S, Serrano-Meneses MA. 2015. Trade-offs in the evolution
563 of bumblebee colony and body size: a comparative analysis. *Ecology and Evolution*
564 5:3914–3926. DOI: 10.1002/ece3.1659.
- 565 Dueñas M-A, Ruffhead HJ, Wakefield NH, Roberts PD, Hemming DJ, Diaz-Soltero H. 2018.
566 The role played by invasive species in interactions with endangered and threatened
567 species in the United States: a systematic review. *Biodiversity and Conservation*
568 27:3171–3183. DOI: 10.1007/s10531-018-1595-x.
- 569 Engler R, Hordijk W, Guisan A. 2012. The MIGCLIM R package – seamless integration of
570 dispersal constraints into projections of species distribution models. *Ecography* 35:872–
571 878. DOI: 10.1111/j.1600-0587.2012.07608.x.

- 572 Escobar LE, Lira-Noriega A, Medina-Vogel G, Peterson AT. 2014. Potential for spread of the
573 white-nose fungus (*Pseudogymnoascus destructans*) in the Americas: use of Maxent and
574 NicheA to assure strict model transference. *Geospatial Health* 9:221–229. DOI:
575 10.4081/gh.2014.19.
- 576 Fujiwara A, Sasaki M, Washitani I. 2016. A scientific note on hive entrance smearing in
577 Japanese *Apis cerana* induced by pre-mass attack scouting by the Asian giant hornet
578 *Vespa mandarinia*. *Apidologie* 47:789–791. DOI: 10.1007/s13592-016-0432-z.
- 579 GBIF.org (07 May 2020) GBIF occurrence download. <https://doi.org/10.15468/dl.kzcg2>.
- 580 Gray L, New A, Science K, Wolfram S. 2003. A mathematician looks at Wolfram’s new kind of
581 science. *Notices of the American Mathematical Society* 50 (2) (2003) 200–211, URL
582 <http://www.ams.org/notices/200302/fea-gray.pdf>. URL
583 <http://www.ams.org/notices/200302/fea-gray.pdf> 50:200–211.
- 584 Hijmans RJ, Etten J van, Sumner M, Cheng J, Bevan A, Bivand R, Busetto L, Canty M, Forrest
585 D, Ghosh A, Golicher D, Gray J, Greenberg JA, Hiemstra P, Hingee K, Geosciences I for
586 MA, Karney C, Mattiuzzi M, Mosher S, Nowosad J, Pebesma E, Lamigueiro OP, Racine
587 EB, Rowlingson B, Shortridge A, Venables B, Wueest R. 2020. *raster: Geographic data*
588 *analysis and modeling*. <https://cran.r-project.org/web/packages/raster/index.html>.
- 589 Hinojosa-Díaz IA, Yáñez-Ordóñez O, Chen G, Peterson AT, Engel MS. 2005. The North
590 American invasion of the giant resin bee (Hymenoptera: Megachilidae). *Journal of*
591 *Hymenoptera Research* 14:69–77.
- 592 Kastberger G, Schmelzer E, Kranner I. 2008. Social waves in Giant Honeybees repel hornets.
593 *PLoS ONE* 3:e3141. DOI: 10.1371/journal.pone.0003141.
- 594 Klingner R, Richter K, Schmolz E, Keller B. 2005. The role of moisture in the nest

- 595 thermoregulation of social wasps. *Naturwissenschaften* 92:427–430. DOI:
596 10.1007/s00114-005-0012-y.
- 597 Li X-D, Liu Z, Zhai Y, Zhao M, Shen H-Y, Li Y, Zhang B, Liu T. 2015. Acute interstitial
598 nephritis following multiple Asian Giant Hornet stings. *American Journal of Case*
599 *Reports* 16:371–373. DOI: 10.12659/AJCR.893734.
- 600 Matsuura M. 1988. Ecological study on Vespine wasps (Hymenoptera: Vespidae) attacking
601 honeybee colonies: 1. Seasonal changes in the frequency of visits to apiaries by Vespine
602 wasps and damage inflicted, especially in the absence of artificial protection. *Applied*
603 *Entomology and Zoology* 23:428–440.
- 604 Matsuura M, Sakagami SF. 1973. A bionomic sketch of the Giant Hornet, *Vespa mandarinia*, a
605 serious pest for Japanese apiculture. *Journal of the Faculty of Science, Hokkaido*
606 *University: Series 6. Zoology* 19:125–162.
- 607 McClenaghan B, Schlaf M, Geddes M, Mazza J, Pitman G, McCallum K, Rawluk S, Hand K,
608 Otis GW. 2019. Behavioral responses of honey bees, *Apis cerana* and *Apis mellifera*, to
609 *Vespa mandarinia* marking and alarm pheromones. *Journal of Apicultural Research*
610 58:141–148. DOI: 10.1080/00218839.2018.1494917.
- 611 Merow C, Smith MJ, Silander JA. 2013. A practical guide to MaxEnt for modeling species'
612 distributions: what it does, and why inputs and settings matter. *Ecography* 36:1058–1069.
613 DOI: 10.1111/j.1600-0587.2013.07872.x.
- 614 Michener CD. 2000. *The Bees of the World*. Baltimore: Johns Hopkins University Press.
- 615 Michener CD. 2007. *The Bees of the World*. Baltimore: Johns Hopkins University Press.
- 616 Monceau K, Bonnard O, Thiéry D. 2014. *Vespa velutina*: a new invasive predator of honeybees
617 in Europe. *Journal of Pest Science* 87:1–16. DOI: 10.1007/s10340-013-0537-3.

- 618 Nuñez-Penichet C, Cobos ME, Peterson AT, Soberón J, Barve N, Barve V, Gueta T. 2020.
619 *biosurvey: Tools for biological survey planning*. <https://github.com/claununez/biosurvey>.
- 620 Ono M, Igarashi T, Ohno E, Sasaki M. 1995. Unusual thermal defense by a honeybee against
621 mass attack by hornets. *Nature* 377:334–336. DOI: 10.1038/377334a0.
- 622 Osorio-Olvera L, Soberón J. 2020. *bam: Species distribution models in the light of the BAM*
623 *theory*. <https://github.com/luismurao/bam>.
- 624 Osorio-Olvera L, Lira-Noriega A, Soberón J, Peterson AT, Falconi M, Contreras-Díaz RG,
625 Martínez-Meyer E, Barve N, Barve V. 2020. NicheToolBox: an R package with a GUI
626 for accessing biodiversity data and modeling and evaluating multidimensional ecological
627 niches. *Methods in Ecology and Evolution* 00:1-8. DOI: 10.1111/2041-
628 210X.13452.Owens HL, Campbell LP, Dornak LL, Saupe EE, Barve N, Soberón J,
629 Ingenloff K, Lira-Noriega A, Hensz CM, Myers CE, Peterson AT. 2013. Constraints on
630 interpretation of ecological niche models by limited environmental ranges on calibration
631 areas. *Ecological Modelling* 263:10–18. DOI: 10.1016/j.ecolmodel.2013.04.011.
- 632 Pearson RG, Raxworthy CJ, Nakamura M, Peterson AT. 2007. Predicting species distributions
633 from small numbers of occurrence records: a test case using cryptic geckos in
634 Madagascar. *Journal of Biogeography* 34(1):102–117.
- 635 Peterson AT, Papeş M, Soberón J. 2008. Rethinking receiver operating characteristic analysis
636 applications in ecological niche modeling. *Ecological Modelling* 213:63–72. DOI:
637 10.1016/j.ecolmodel.2007.11.008.
- 638 Phillips SJ, Anderson RP, Dudík M, Schapire RE, Blair ME. 2017. Opening the black box: an
639 open-source release of Maxent. *Ecography* 40:887–893. DOI: 10.1111/ecog.03049.
- 640 Phillips SJ, Anderson RP, Schapire RE. 2006. Maximum entropy modeling of species

- 641 geographic distributions. *Ecological Modelling* 190:231–259. DOI:
642 10.1016/j.ecolmodel.2005.03.026.
- 643 Pimentel D, Zuniga R, Morrison D. 2005. Update on the environmental and economic costs
644 associated with alien-invasive species in the United States. *Ecological Economics*
645 52:273–288. DOI: 10.1016/j.ecolecon.2004.10.002.
- 646 Pyšek P, Richardson DM. 2010. Invasive species, environmental change and management, and
647 health. *Annual Review of Environment and Resources* 35:25–55. DOI: 10.1146/annurev-
648 environ-033009-095548.
- 649 Quezada-Euán JJG, Nates-Parra G, Maués MM, Roubik DW, Imperatriz-Fonseca VL. 2018. The
650 economic and cultural values of stingless bees (Hymenoptera: Meliponini) among ethnic
651 groups of tropical America. *Sociobiology* 65:534–557. DOI:
652 10.13102/sociobiology.v65i4.3447.
- 653 R Core Team. 2019. *R: A language and environment for statistical computing*. Vienna, Austria:
654 R Foundation for Statistical Computing.
- 655 Schmidt JO, Yamane S, Matsuura M, Starr CK. 1986. Hornet venoms: lethality and lethal
656 capacities. *Toxicon* 24:950–954. DOI: 10.1016/0041-0101(86)90096-6.
- 657 Simões M, Romero-Alvarez D, Nuñez-Penichet C, Jiménez L, Cobos ME. 2020. General theory
658 and good practices in ecological niche modeling: a basic guide. *Biodiversity Informatics*
659 15:67–68.
- 660 Smith-Pardo AH, Carpenter JM, Kimsey L. 2020. The diversity of hornets in the genus *Vespa*
661 (Hymenoptera: Vespidae; Vespinae), their importance and interceptions in the United
662 States. *Insect Systematics and Diversity* 4:1–27.
- 663 Sugahara M, Nishimura Y, Sakamoto F. 2012. Differences in heat sensitivity between Japanese

- 664 honeybees and hornets under high carbon dioxide and humidity conditions inside bee
665 balls. *Zoological Science* 29:30–36. DOI: 10.2108/zsj.29.30.
- 666 Sunday JM, Bates AE, Dulvy NK. 2012. Thermal tolerance and the global redistribution of
667 animals. *Nature Climate Change* 2:686–690. DOI: 10.1038/nclimate1539.
- 668 Vega GC, Pertierra LR, Olalla-Tárraga MÁ. 2018. MERRAclim, a high-resolution global dataset
669 of remotely sensed bioclimatic variables for ecological modelling. *Scientific Data*
670 4:170078. DOI: 10.1038/sdata.2017.78.
- 671 Viana JL, Sousa H de AC, Alves RM de O, Pereira DG, Silva Jr. JC, Paixão JF da, Waldschmidt
672 AM, Viana JL, Sousa H de AC, Alves RM de O, Pereira DG, Silva Jr. JC, Paixão JF da,
673 Waldschmidt AM. 2015. Bionomics of *Melipona mondury* Smith 1863 (Hymenoptera:
674 Apidae, Meliponini) in relation to its nesting behavior. *Biota Neotropica* 15. DOI:
675 10.1590/1676-06032015009714.
- 676 Vilà M, Espinar JL, Hejda M, Hulme PE, Jarošík V, Maron JL, Pergl J, Schaffner U, Sun Y,
677 Pyšek P. 2011. Ecological impacts of invasive alien plants: a meta-analysis of their
678 effects on species, communities and ecosystems. *Ecology Letters* 14:702–708. DOI:
679 10.1111/j.1461-0248.2011.01628.x.
- 680 Warren DL, Seifert SN. 2011. Ecological niche modeling in Maxent: the importance of model
681 complexity and the performance of model selection criteria. *Ecological Applications*
682 21:335–342. DOI: 10.1890/10-1171.1.
- 683 Wilcove DS, Rothstein D, Dubow J, Phillips A, Losos E. 1998. Quantifying threats to imperiled
684 species in the United States. *BioScience* 48:607–615. DOI: 10.2307/1313420.
- 685 Yanagawa Y, Morita K, Sugiura T, Okada Y. 2007. Cutaneous hemorrhage or necrosis findings
686 after *Vespa mandarinia* (wasp) stings may predict the occurrence of multiple organ

687 injury: a case report and review of literature. *Clinical Toxicology* 45:803–807. DOI:
688 10.1080/15563650701664871.

689 Zhu G, Illan JG, Looney C, Crowder DW. 2020. Assessing the ecological niche and invasion
690 potential of the Asian giant hornet. *Proceedings of the National Academy of Sciences*
691 *USA*. DOI: 10.1073/pnas.2011441117.

692 Zurell D, Franklin J, König C, Bouchet PJ, Dormann CF, Elith J, Fandos G, Feng X,
693 Guillera-Arroita G, Guisan A, Lahoz-Monfort JJ, Leitão PJ, Park DS, Peterson AT,
694 Rapacciuolo G, Schmatz DR, Schröder B, Serra-Diaz JM, Thuiller W, Yates KL,
695 Zimmermann NE, Merow C. 2020. A standard protocol for reporting species distribution
696 models. *Ecography*. DOI: 10.1111/ecog.04960.

697 **Tables**

698 Table 1. Summary of results of ecological niche modeling for *Vespa mandarinia*, including
699 model calibration, model evaluation, and relevant Maxent settings for models selected after
700 independent testing. Maxent settings are represented in the columns ‘Regularization multiplier,’
701 ‘Feature classes,’ and ‘Variable sets’. The column ‘Calibration processes’ refers to each of the
702 five calibrations processes that were done with different sets of random points, for every
703 calibration scheme. The variables included in the sets mentioned on this table can be found in
704 Table 1S-2S. E: free extrapolation; EC: extrapolation with clamping; NE: no extrapolation, PCs:
705 principal components.

706 **Figures**

707 Figure 1. Hypothesis of accessible areas (**M**) and representation of the occurrence records of
708 *Vespa mandarinia* across its native distribution. The three panels represent the occurrences left
709 after cleaning (A) and after applying the two thinning approaches (B and C).

710 Figure 2. Schematic representation of methods used to obtain ecological niche models for *Vespa*
711 *mandarinia*. The aim of the modeling process was to consider the variability resulting from
712 different procedures and methodological decisions made during model calibration.

713 Figure 3. Median of potentially suitable areas for *Vespa mandarinia* predicted with free
714 extrapolation for different calibration schemes in the calibration area (left panels) and in North
715 America (right panels). Only models that anticipated the invaded areas of North America were
716 included. The color pallet is standard for all figure panels.

717 Figure 4. Sum of all suitable areas for *Vespa mandarinia* in North America derived from
718 binarizing each replicate of selected models (model transfers done with extrapolation) using a
719 5% threshold. Each replicate predicted the known invaded localities of this hornet.

720 Figure 5. Agreement of areas with extrapolation risk for models of *Vespa mandarinia* in North
721 America, separated by calibration schemes.

722 Figure 6. Results from simulations of the potential dynamics of invasion of *Vespa mandarinia* in
723 North America. Dark shades of green show areas that the species reached in a high percentage of
724 scenarios, while light shades of green represent areas reached only rarely by the species. Arrows
725 represent the general path of potential invasion.

726 Figure 7. Representation of potential ecological and economic impacts of an invasion of *Vespa*

727 *mandarina*. Top panel: honey production (in US dollars) in Mexico and the United States in
728 2016. Bottom panel: species richness of the genera *Bombus* (bumble bees) and *Melipona*
729 (stingless bees) in North America. The area shaded in gray represents the simulated potential
730 invaded area of *Vespa mandarina* in North America obtained with the 50 km spatial thinning
731 occurrences and PCs as environmental predictors. We used this scenario because is the one that
732 best connects the known invaded areas with the eastern United States.

Figure 1

Hypothesis of accessible areas (M) and representation of the occurrence records of *Vespa mandarinia* across its native distribution.

The three panels represent the occurrences left after cleaning (A) and after applying the two thinning approaches (B and C).

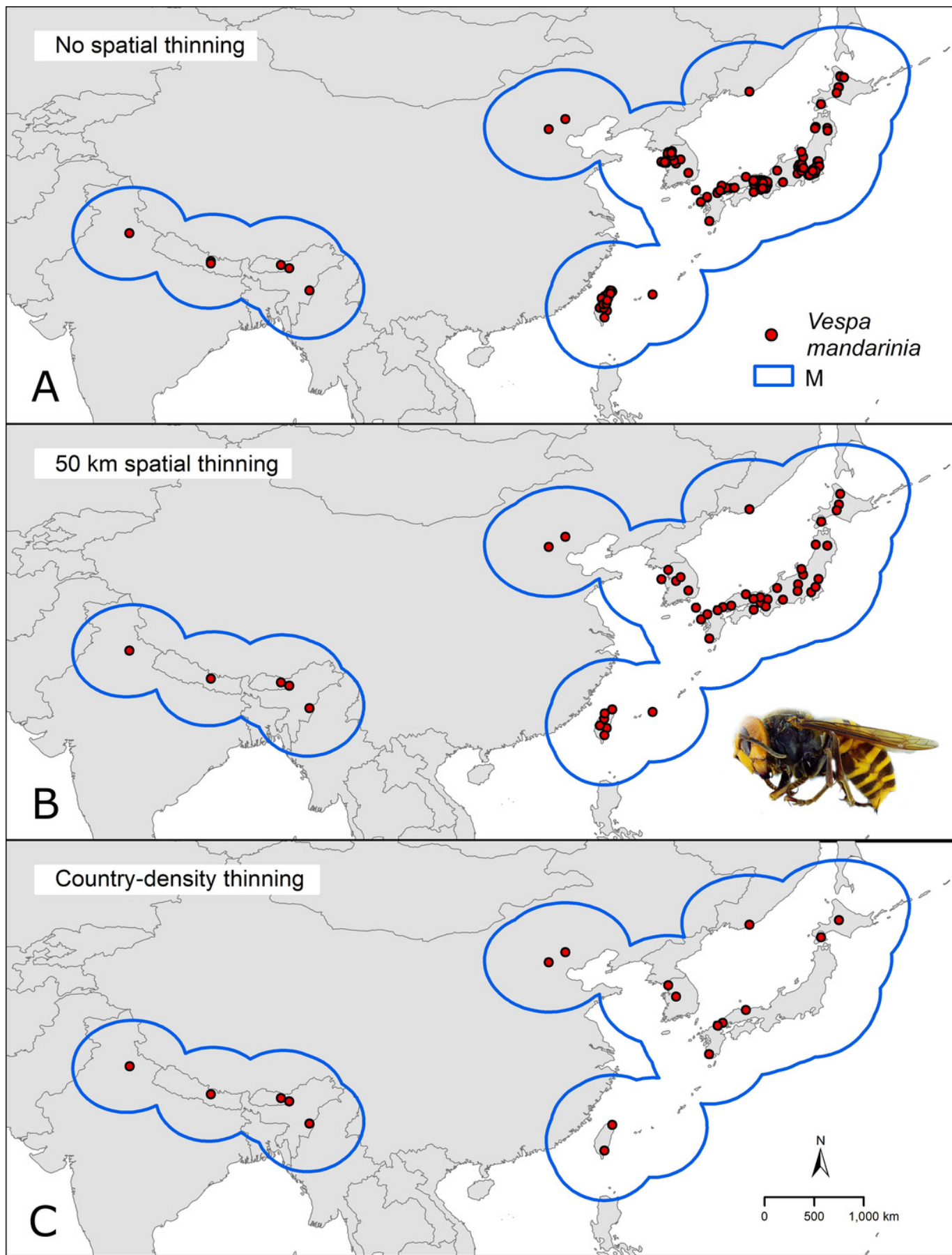


Figure 2

Schematic representation of methods used to obtain ecological niche models for *Vespa mandarinia*.

The aim of the modeling process was to consider the variability resulting from different procedures and methodological decisions made during model calibration.

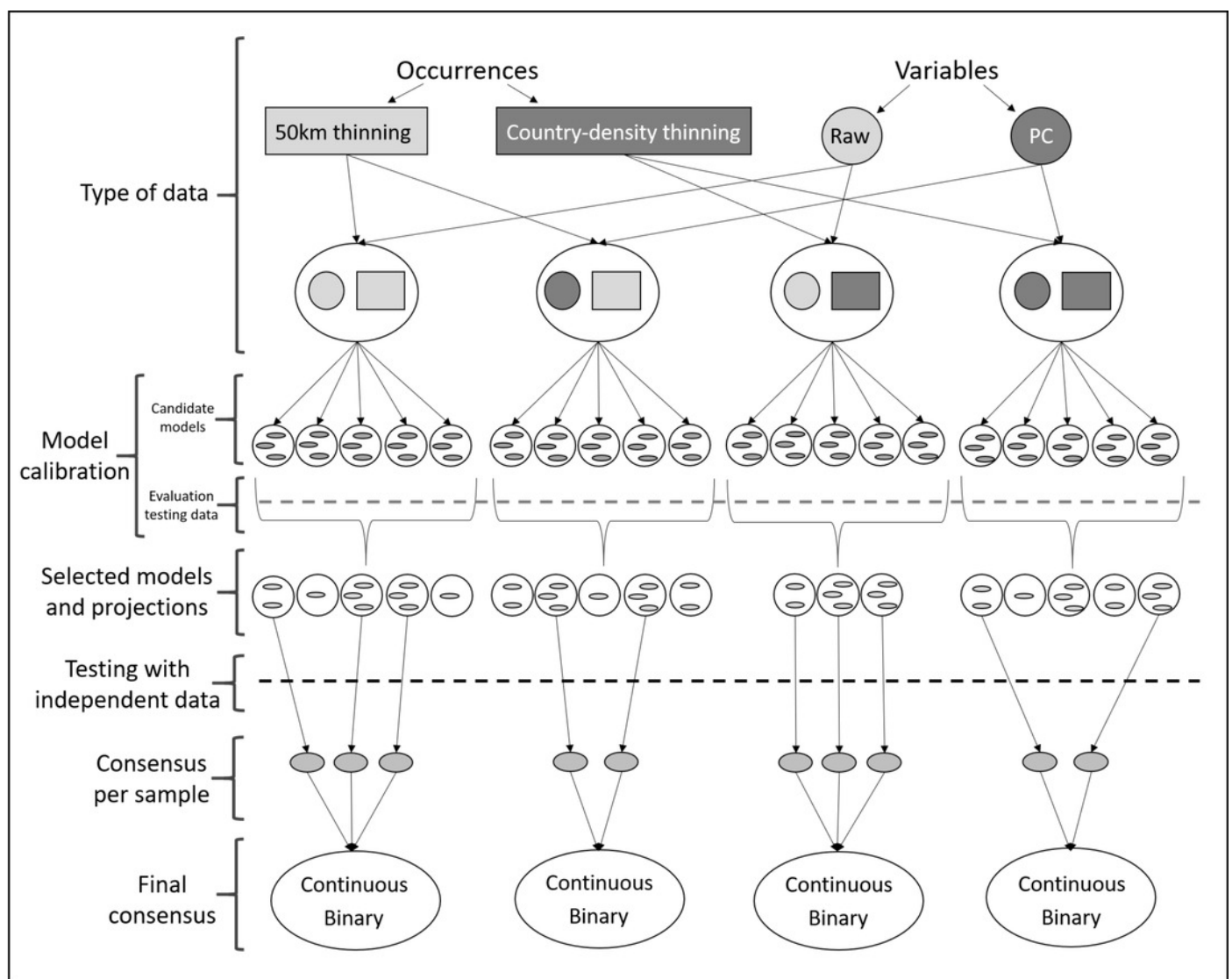


Figure 3

Median of potentially suitable areas for *Vespa mandarinia* predicted with free extrapolation for different calibration schemes in the calibration area (left panels) and in North America (right panels).

Only models that anticipated the invaded areas of North America were included. The color pallet is standard for all figure panels.

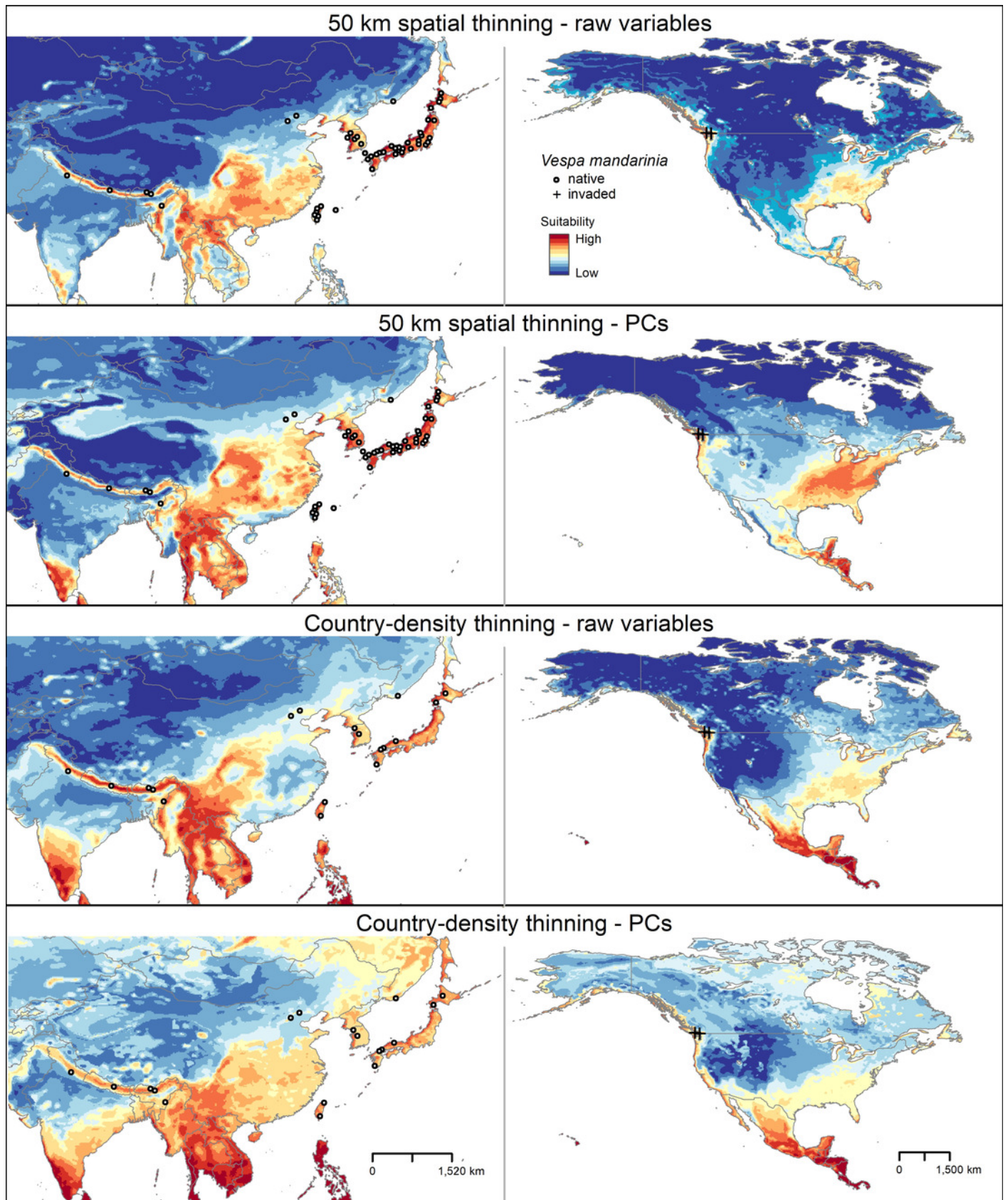


Figure 4

Sum of all suitable areas for *Vespa mandarinia* in North America derived from binarizing each replicate of selected models (model transfers done with extrapolation), using a 5% threshold.

Each replicate predicted the known invaded localities of this hornet.

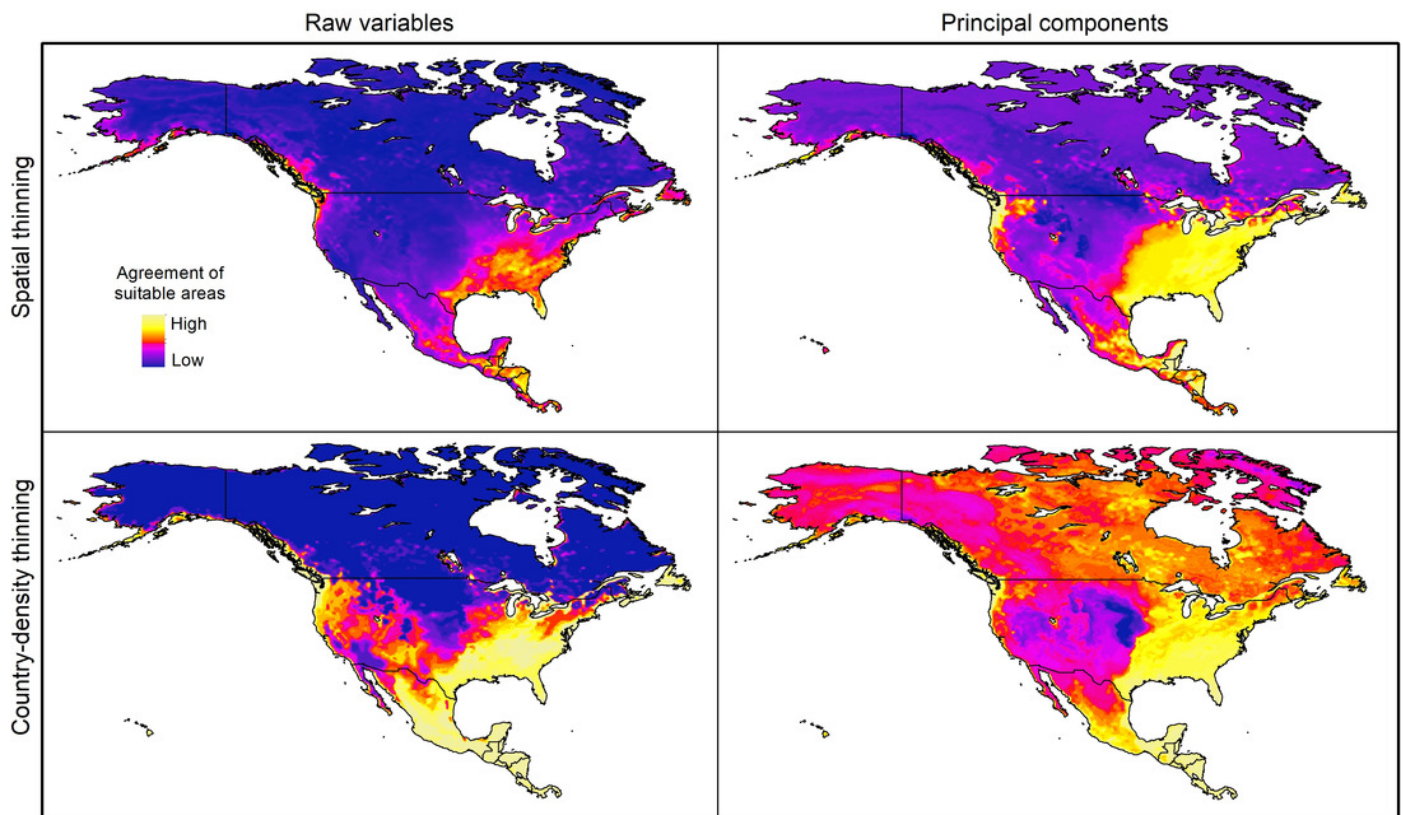


Figure 5

Agreement of areas with extrapolation risk for models of *Vespa mandarinia* in North America, separated by calibration schemes.

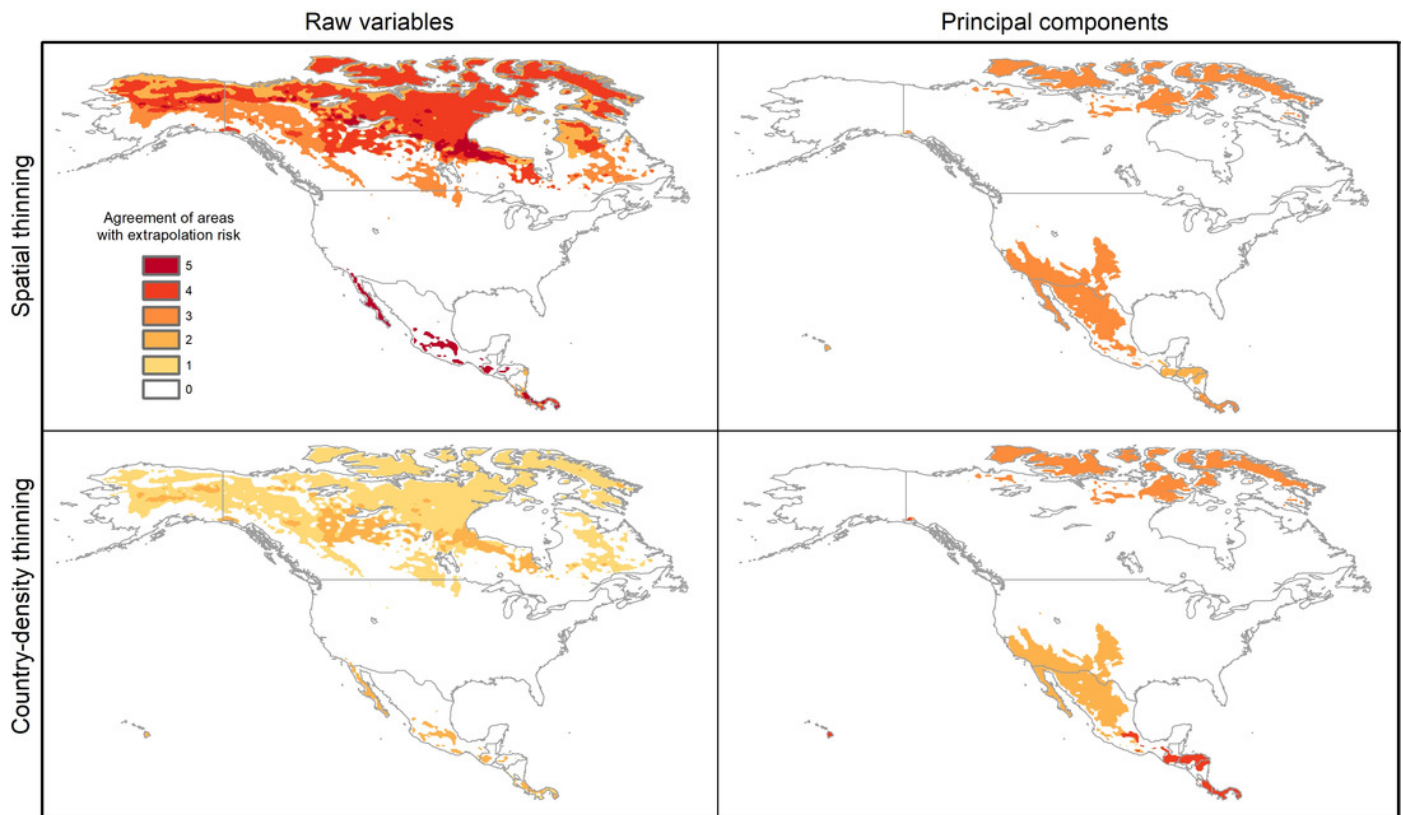


Figure 6

Results from simulations of the potential dynamics of invasion of *Vespa mandarinia* in North America.

Dark shades of green show areas that the species reached in a high percentage of scenarios, while light shades of green represent areas reached only rarely by the species. Arrows represent the general path of potential invasion.

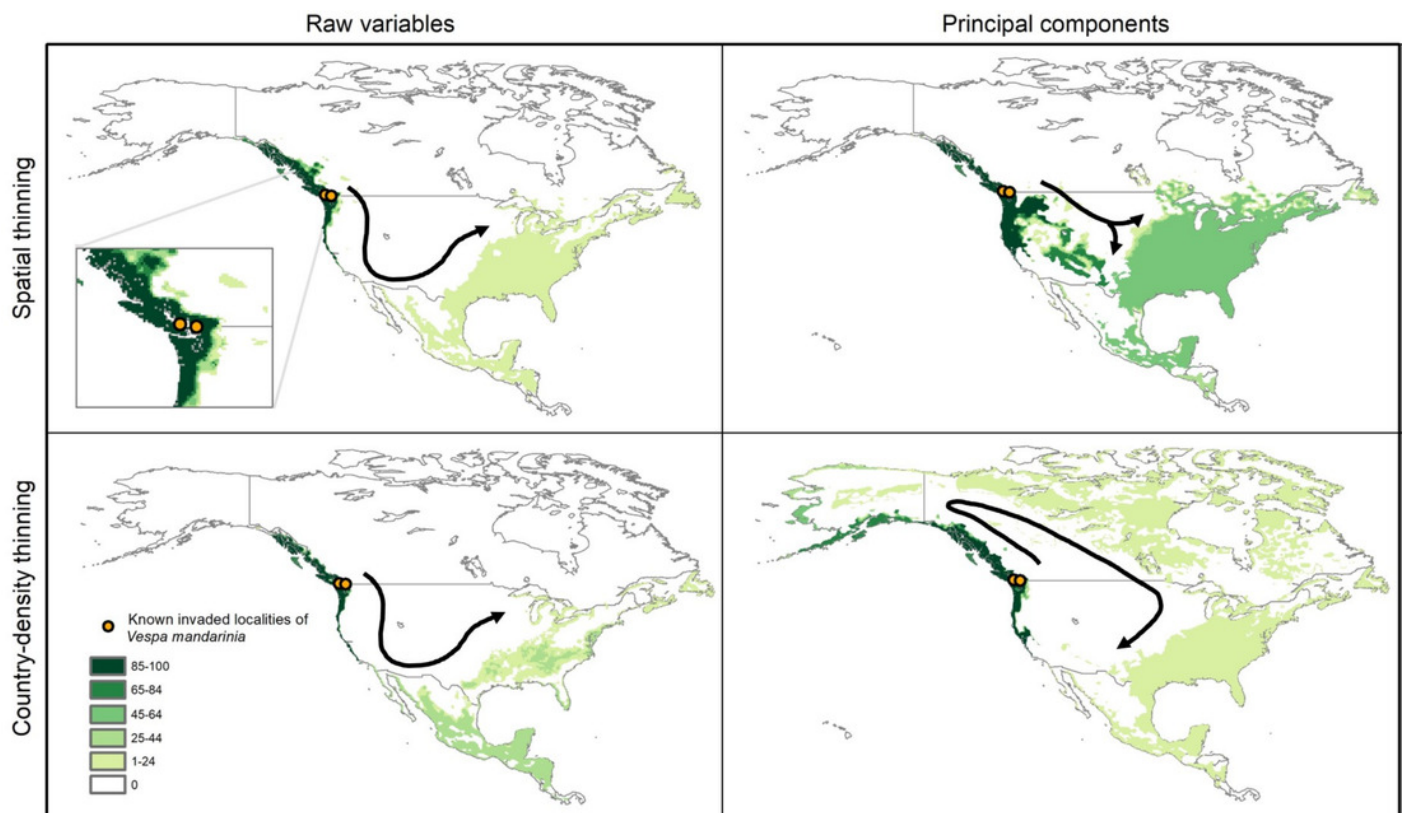


Figure 7

Representation of potential ecological and economic impacts of an invasion of *Vespa mandarinia*.

Top panel: honey production (in US dollars) in Mexico and the United States in 2016. Bottom panel: species richness of the genera *Bombus* (bumble bees) and *Melipona* (stingless bees) in North America. The area shaded in gray represents the simulated potential invaded area of *Vespa mandarinia* in North America obtained with the 50 km spatial thinning occurrences and PCs as environmental predictors. We used this scenario because is the one that best connects the known invaded areas with the eastern United States.

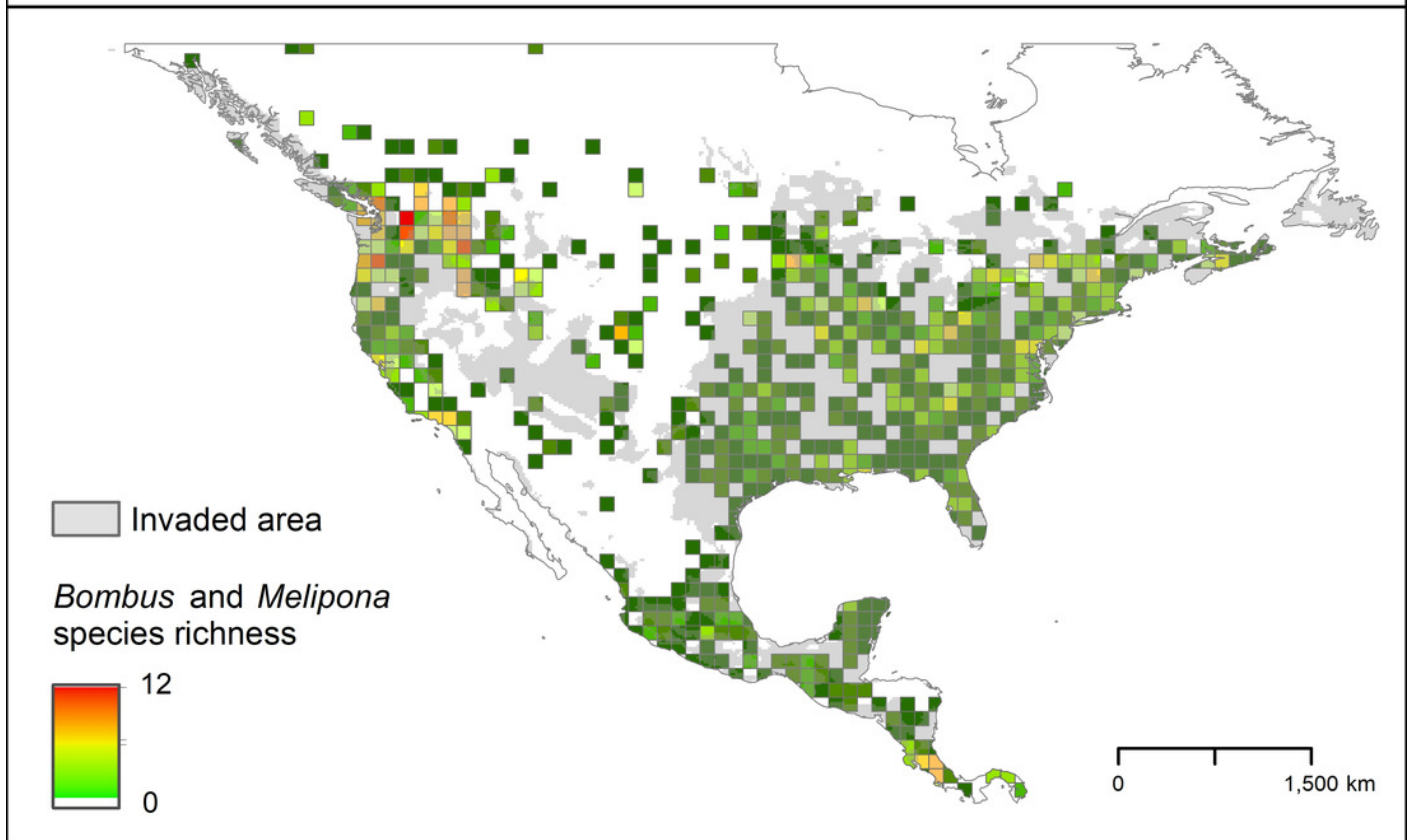
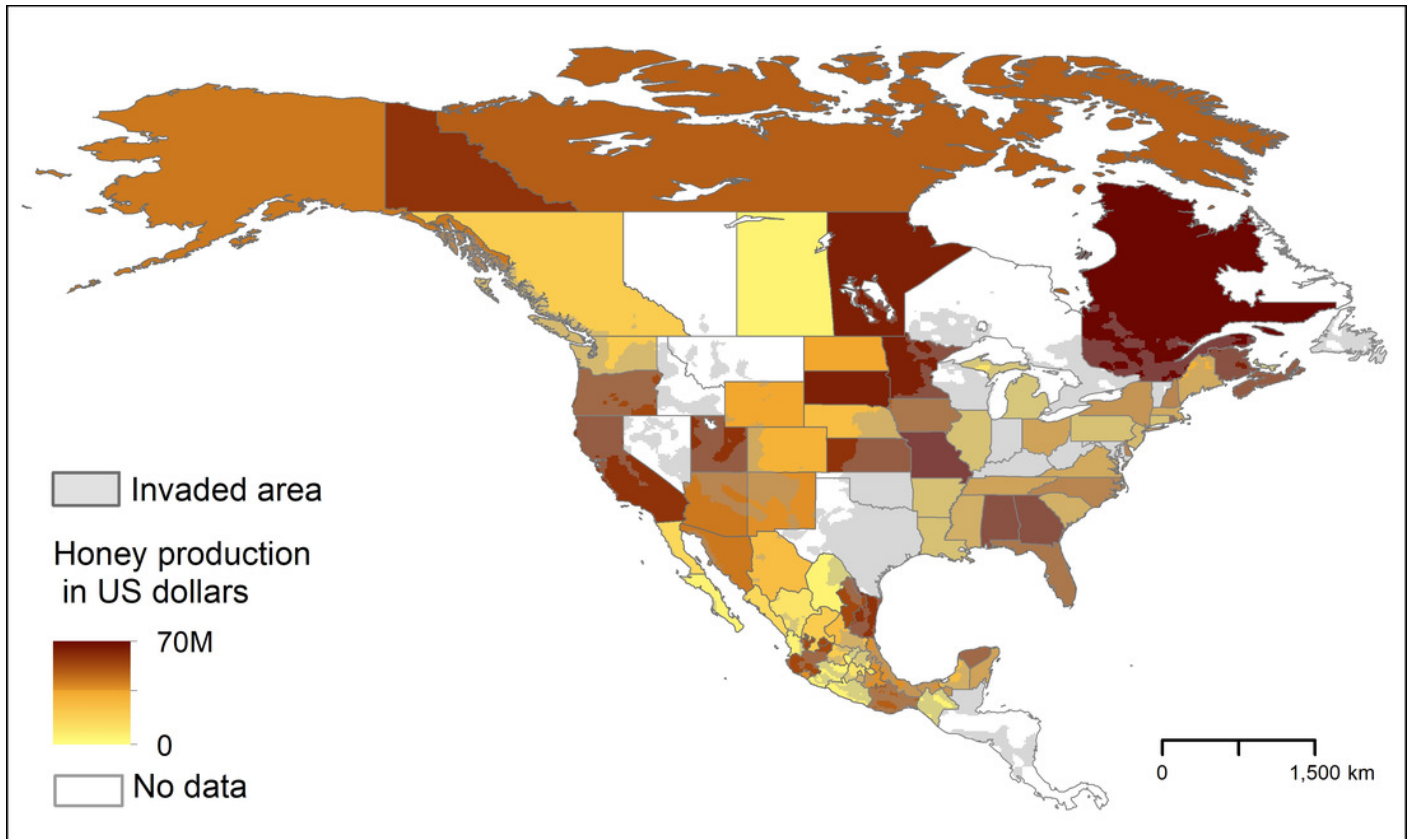


Table 1 (on next page)

Summary of results of ecological niche modeling for *Vespa mandarinia*, including model calibration, model evaluation, and relevant Maxent settings for models selected after independent testing.

Maxent settings are represented in the columns 'Regularization multiplier,' 'Feature classes,' and 'Variable sets'. The column 'Calibration processes' refers to each of the five calibrations processes that were done with different sets of random points, for every calibration scheme. The variables included in the sets mentioned on this table can be found in Table 1S-2S. E: free extrapolation; EC: extrapolation with clamping; NE: no extrapolation, PCs: principal components.

Calibration scheme	Calibration processes	Models meeting selection criteria	Models predicting independent records (E; EC; NE)	Regularization multiplier	Feature classes	Variable sets
Raw variables and distance thinned occurrences	1	6	8; 2; 10	0.25; 0.5; 0.75	lq; lqpt	42; 43; 50; 51; 57
	2	1	-	-	-	-
	3	1	6; 4; 4	0.75	lqpth	12
	4	1	2; -; 1	0.25	lq	21
	5	2	7; 7; 13	0.1; 0.25	lq	26
PCs and distance thinned occurrences	1	4	24; 18; 20	5	lqph; lqpth	7; 11
	2	2	10; 5; 5	0.25; 0.5	qp	11
	3	4	22; 23; 19	0.1; 0.25; 0.5; 0.75	lp	11
	4	3	9; 8; 11	0.25; 0.5; 0.75	qp	7
	5	6	21; 21; 26	0.1; .25; 0.5; 0.75	lqp	2; 9
Raw variables and country-density thinned occurrences	1	1	4; 4; 6	0.1	lqp	22
	2	2	4; 11; 8	0.1	lq; lqp	5; 22
	3	-	-	-	-	-
	4	3	15; 13; 16	0.1; 2	lq; lqph; lqpth	13; 32
	5	-	-	-	-	-
PCs and country-density thinned occurrences	1	7	32; 31; 32	0.25; 0.5; 0.7; 1	lp; lqpt; lqpth	2; 4; 5; 6; 8
	2	1	1; 3; 1	1	lqpth	8
	3	1	5; 6; 7	0.1	q	4
	4	4	24; 22; 18	0.1; 0.25; 0.5; 0.74	lp	1
	5	2	5; 7; 5	1	lqp	1; 6

1

2